Biogeosciences
Discussions

Open Access

Wind driven changes in the ocean carbon sink

N. C. Swart[1], J. C. Fyfe[1], O. A. Saenko[1], and M. Eby[2]

[1]Canadian Centre for Climate Modelling and Analysis, University of Victoria, P.O. Box 1700 STN CSC, Victoria, BC, V8W 2Y2, Canada
[2]School of Earth and Ocean Sciences, University of Victoria, Victoria, BC, Canada

Correspondence to: N. C. Swart (neil.swart@ec.gc.ca)

Abstract

We estimate the historical ocean carbon sink over 1871 to 2010 using an ocean bio-geochemical model driven with observed wind forcing. We focus on the influence of wind and mesoscale eddy changes on the net surface CO_2 flux, which are most significant after 1950. The observed wind changes act to reduce the annual ocean carbon sink by 0.009 to 0.023 $Pg\,yr^{-1}\,decade^{-1}$ over 1950 to 2010, and are consistent with previous studies covering only the latter part of the 20th century. The response of the ocean circulation and the carbon cycle to wind changes is sensitive to the parameterization of mesoscale eddies in our coarse resolution simulations. With a variable eddy transfer coefficient, eddy activity in the Southern Ocean increases in response to intensifying historical winds, partially compensating for direct wind-driven circulation changes. Thus with a variable eddy transfer coefficient the response to wind changes is about 2.5 times smaller than when using a constant coefficient. Finally, we show by comparing six reanalyses over 1980 to 2010 that estimated historical wind trends differ significantly. Through simulations forced with these reanalysis winds we show that the influence of historical wind changes on ocean carbon uptake is highly uncertain and depends on the choice of surface wind forcing product.

1 Introduction

Estimates of historical ocean carbon uptake by ocean biogeochemical models are a central constraint in our understanding of the global carbon cycle (Le Quéré et al., 2013; Wanninkhof et al., 2013; Sarmiento et al., 2010). The rate of simulated ocean carbon uptake in such models is sensitive to trends in the surface wind forcing, particularly over the Southern Ocean. Several previous ocean model studies, forced at the surface by reanalysis winds, have suggested that the historical intensification of the Southern Hemisphere westerlies has reduced the Southern Ocean CO_2 sink (e.g. Le Quéré et al., 2007; Lovenduski et al., 2007). The intensified winds reduce the CO_2 sink

by increasing the Southern Ocean residual overturning circulation and therefore the rate of outgassing of natural CO_2 (Lovenduski et al., 2008).

However, significant uncertainties exist in previous model based estimates of the wind feedback on historical ocean carbon uptake. Firstly, the previous studies have primarily used NCEP Reanalysis 1 (R1) to derive the surface wind forcing, limiting them to the period after 1948. The influence of wind changes prior to 1948 remains unknown. Secondly, the wind-induced circulation changes are modulated by ocean eddies (Lovenduski et al., 2013; Böning et al., 2008) which are not resolved nor adequately parameterized in many studies using coarse resolution models (e.g. Lovenduski et al., 2008; Le Quéré et al., 2007). Finally, the historical wind changes are themselves uncertain, as evidenced by differences amongst trends over 1980 to 2010 in the available reanalyses (Swart and Fyfe, 2012).

The wind induced increase in outgassing of natural CO_2 from the Southern Ocean is also offset by an enhanced uptake of anthropogenic CO_2 driven by the rising atmospheric concentrations, though which process dominates is subject to debate (Le Quéré et al., 2010; Zickfeld et al., 2008). The resulting net trend in historical Southern Ocean uptake remains uncertain (Lenton et al., 2013), but it is of key interest given the primary importance of the region for anthropogenic CO_2 uptake (Wanninkhof et al., 2013; Gruber et al., 2009).

Here we work to address the uncertainties in the wind feedback on ocean carbon uptake. We use the 20th Century Reanalysis version 2 (20CR, Compo et al., 2011) to produce a model based estimate of historical ocean carbon uptake since 1871. First we examine the influence of time evolving wind changes on surface carbon fluxes. Next we test the sensitivity of the wind-induced changes in circulation and surface fluxes to the type of eddy parameterization. Finally we show how differences in wind changes among six reanalyses influence the wind feedback on carbon uptake over the period 1980 to 2010.

Full Screen / Esc

Printer-friendly Version

Interactive Discussion

2   Data and methods

2.1   The UVic Earth System Climate Model

We use version 2.9 of the University of Victoria Earth System Climate Model (UVic ESCM), which is an Earth System Model of Intermediate Complexity described by Weaver et al. (2001). The UVic ESCM has a fully dynamic 3-D ocean general circulation model, coupled to a vertically integrated energy-moisture balance (EMB) atmosphere model and a thermodynamic-dynamic sea ice model (Weaver et al., 2001). All the model components share a global domain with a horizontal resolution of 3.6° longitude by 1.8° latitude, and there are 19 vertical levels in the ocean.

The UVic ESCM also incorporates a state of the art carbon cycle, which produces realistic distributions of dissolved inorganic carbon (DIC) and alkalinity in the ocean (Eby et al., 2009; Schmittner et al., 2008), realistic surface fluxes of CO_2 (Eby et al., 2009) and can reproduce historical ocean carbon uptake to within observational uncertainty (Eby et al., 2013, 2009).

In the default version of the UVic ESCM, mesoscale ocean eddies are represented via the Gent–McWilliams (GM) eddy parameterization (Gent and McWilliams, 1990), which has a constant eddy transfer coefficient of $800\,\mathrm{m}^2\,\mathrm{s}^{-1}$. Here we have also implemented a variable eddy transfer coefficient. In this formulation, which follows Gnanadesikan et al. (2006) and Farneti and Gent (2011), the GM eddy transfer coefficient is allowed to vary in space and time and is prescribed as:

$$K_{GM}(x,y,t) = \frac{\alpha}{h - h_m} \int_{-h}^{-h_m} |\nabla\rho|\,dz \left(\frac{gL^2}{\rho_0 N_0}\right) \tag{1}$$

where g is the gravitational acceleration, $\rho_0 = 1025\,\mathrm{kg\,m}^{-3}$ is a constant reference density, N_0 is a prescribed constant buoyancy frequency of $0.004\,\mathrm{s}^{-1}$, L is a constant prescribed eddy length scale of 50 km, α is a dimensionless tuning constant set to 1, and

$|\nabla\rho|$ is the horizontal density gradient or baroclinicity which is averaged over depths between $h_m = 100\,m$ and $h = 2000\,m$. The range of K_{GM} is then constrained between a minimum of 300 and a maximum of $5000\,m^2\,s^{-1}$. For each experiment described below, one version is conducted with the constant GM coefficient and a second version is conducted with the variable GM formulation.

2.2 Experimental design

Due to the simplified nature of the UVic ESCM's atmosphere, ocean surface wind-stress and wind-speed fields are specified, but the surface buoyancy flux is computed prognostically. The model was equilibrated for over 10 000 years with year 1800 forcing (greenhouse gas, sulphate aerosol, land-use, orbital, solar) using surface wind speed and wind stress climatologies derived from 20CR over the years 1871 to 1899. 20CR is an ensemble reanalysis, and we use the ensemble mean monthly wind fields. Then, transient simulations were run for the period 1800 to 2010 under historical forcing.

Two sets of transient runs were conducted under 20CR winds. In FIXED the radiative forcing evolved in time but the winds were held fixed by using repeating monthly winds from 1871. In TRANSIENT the winds evolved according to 20CR monthly winds from 1871 onwards. The influence of wind changes on surface CO_2 fluxes is computed as TRANSIENT minus FIXED.

An additional set of simulations was done to compare wind changes in six different reanalyses for the 1980 to 2010 period during which they all overlap (Table 1). For each reanalysis, the model was run for the period 1800 to 1980 with monthly repeating 1980 winds, and evolving radiative forcing. At year 1980 the simulations were branched in two: the first continued with repeating 1980 winds, while in the second the winds evolved monthly in time from 1980 to 2010.

2.3 Trends and significance

We calculate linear least-squares trends for the surface wind and CO_2 flux fields. The confidence interval of the trends is calculated from the standard error of the estimate multiplied by the 5 % cutoff value of the student-t distribution with $n - 2$ degrees of freedom, where n is the length of the record. Trends are considered significant (Table 2) if the associated p value is less than 0.05.

3 The influence of wind and eddy changes since 1871

3.1 Climatology and changes in 20CR winds

The most prominent trends in the 20CR winds occur in the region of the Southern Hemisphere (SH) westerlies (Fig. 1). In the zonal mean, the SH westerly jet shows variability in its strength up until about 1950, indicated by positive and negative departures from the climatology (Fig. 1b). From around 1950 to 2010 there is additionally a significant intensification of the jet, with the zonal-mean stress increasing by about 25 % over this period. This strengthening of the westerly jet is consistent with previous results (Swart and Fyfe, 2012) and is attributable to a combination of ozone and greenhouse gas forcing (Son et al., 2010; Thompson and Solomon, 2002).

Ocean biogeochemical models have shown that changes in the westerly wind jet can influence the surface CO_2 flux, but previous simulations have been confined to the latter part of the twentieth century. 20CR is currently the best available estimate of the evolution of ocean surface winds in the pre-satellite era. We note that uncertainties exist in the 20CR winds, particularly in the Southern Hemisphere during the early part of the reanalysis when constraining observational data was sparse (Compo et al., 2011). We will consider the effect of wind uncertainty in Sect. 4. But first we will consider the influence of wind changes on surface CO_2 fluxes since 1871 by forcing the UVic ESCM with 20CR winds.

3.2 Changes in surface fluxes and carbon uptake

We first consider the TRANSIENT simulations which have time-evolving winds and atmospheric CO_2 concentrations which increase according to observations from about 284 ppm in 1800 to 387 ppm in 2010. The simulated net sea to air CO_2 flux increases in magnitude in response to these rising atmospheric concentrations (Fig. 2a). The simulated net fluxes fall within observational estimates for the three decades of the 1980's, 1990's and 2000's (Ciais et al., 2013). The fluxes are generally similar, though not identical, in the simulations with a constant and a variable eddy transfer coefficient.

Our primary interest lies in the influence of the 20CR wind changes on the net surface CO_2 flux. To consider this we compute the difference in the net surface fluxes between the TRANSIENT simulation and the FIXED simulation (Fig. 2b). The wind changes result in a negative sea to air CO_2 flux anomaly from 1871 to about 1900, implying an enhanced oceanic carbon sink, which is followed by a brief but large positive anomaly. The flux anomalies over this period are associated with wind variability, particularly the large reduction in zonal wind-stress near 60° S which occurred around 1883. The timing of this anomaly is coincident with the eruption of Krakatoa, which may have influenced the winds though aerosol effects. Following this initial variability the net flux anomaly remained close to zero on average between about 1920 and 1950.

From around 1950 onwards the wind changes result in a positive sea to air CO_2 flux anomaly on average, indicating a weakened ocean sink (Fig. 2b). The positive trend in the wind induced surface flux anomaly over 1950 to 2010 is significant at the 5 % level under the constant GM scheme (Table 2) and is also coincident with the intensification of the SH westerlies. Previous studies have reported similar trends in the surface CO_2 flux due to wind forcing with a constant GM eddy paramterization (Le Quéré et al., 2010, 2007; Lovenduski et al., 2008), but these estimates only covered the latter part of the 20th and early 21st century. Here we have considered wind changes over 1871 to 2010 which in total reduce the ocean carbon sink by between 8.3 and 9.5 Pg, relative to the simulations with fixed winds.

The multidecadal trends are sensitive to the time period selected because of the large interannual variability in the fluxes (Wanninkhof et al., 2013; Lenton et al., 2013), and because the wind speed trend accelerates in time. To see this we calculated rolling trends over a period with a start-year which rolls forward from 1871 to 1990 and an end year of 2010 (Fig. 3). That is, the trend for 1871 is calculated over 1871 to 2010, while the trend for 1872 is calculated from 1872 to 2010 and so on until 1990. Significant trends in the surface flux anomaly only emerge above the interannual variability for trends starting before about 1980 (periods > 30 years). Conversely, flux anomaly trends starting after 1980 (period < 30 years) are strongly influenced by internal variability and are not significant. Our long time-series allows us to identify the positive trend in the surface flux anomaly due to wind changes with a high degree of confidence ($p < 0.001$) not attainable with shorter records. Using the rolling trends it can also be seen that as the Southern Ocean wind-speed trends accelerate after 1960 (Fig. 3a), so do the positive trends in the surface flux anomalies.

The surface flux response to wind changes is also sensitive to the parameterization of mesoscale eddies. Between 1950 and 2010 the linear trend in the wind-induced surface flux anomaly was 2.5 times higher under the constant GM scheme than under the variable GM scheme, at 0.023 and 0.009 $Pg\,yr^{-1}\,decade^{-1}$ respectively (Table 2). The flux anomaly trends in the simulations using the constant and variable GM scheme are significantly different at the 5 % level, regardless of the period over which the trends are calculated (Fig. 3b). Most previous studies on the influence of wind changes on the ocean carbon sink have used a constant GM scheme (Le Quéré et al., 2010, 2007; Lovenduski et al., 2008). Our simulations highlight the importance of eddy parameterization in determining the magnitude of diagnosed wind feedback on ocean carbon uptake.

The difference in the time-cumulative surface fluxes by latitude indicates that the largest CO_2 loss from the ocean due to wind changes occurs in the Southern Ocean between 40° and 60° S (Fig. 4a). The difference in the fluxes between the variable and constant GM simulations shows that the eddies also principally modulate the response

Full Screen / Esc

Printer-friendly Version

Interactive Discussion

to the wind changes in the Southern Ocean (Fig. 4b). Specifically, the region between 40° and 50° S shows a negative flux anomaly indicating that the intensifying westerlies cause less oceanic outgassing in the variable GM scheme than in the constant GM scheme. The subdued response to wind forcing in the variable GM scheme is due to compensating changes in the wind and eddy driven Southern Ocean overturning circulation which we now examine.

3.3 Changes in eddies and the meridional overturning circulation

The difference in the zonal-mean eddy transfer coefficient between the TRANSIENT and FIXED variable GM simulations shows that the eddy coefficient responded to the surface wind forcing (Fig. 5a). The most prominent change was an increase in the eddy coefficient in the region between 40° and 50° S, with the strongest increase occurring after 1950. The eddy coefficient influences the surface carbon fluxes by modulating the residual overturning circulation. Above topography at the latitudes of Drake Passage the Southern Ocean residual meridional overturning streanfunction can be approximately represented as:

$$\Psi_r = -\frac{\tau_x}{\rho f} + K_{\mathrm{GM}} S_b \tag{2}$$

where τ_x is the zonal wind stress, ρ is the density, f is the Coriolis parameter, K_{GM} is the eddy transfer coefficient and S_b is the slope of isopycnal surfaces (Marshall and Radko, 2003). The first term on the right represents the Eulerian mean (wind driven) circulation and the second term represents the eddy induced circulation, which tends to oppose the mean flow.

In our simulations the intensifying westerlies act to increase the rate of the residual overturning circulation through the Eulerian mean component (Fig. 5b). The trend in the MOC is significant at around 1.0 Sv decade^{-1} (1 Sv = 1×10^6 m^3 s^{-1}) in the constant GM run where the eddy coefficient is held fixed. In the case of the variable GM scheme, the concomitant increase in the eddy transfer coefficient (Fig. 5a) leads to an increase

in the eddy induced circulation, which partially compensates for the wind-induced increase in the Eulerian mean circulation[1]. The net effect is that the wind forced trend in the residual overturning circulation is about 2.5 times smaller (0.37 Sv decade^{-1}) in the variable GM simulations. The partial eddy compensation that occurs in our variable GM simulations is in agreement with recent theoretical predictions (Meredith et al., 2011), eddy resolving model simulations (Morrison and Hogg, 2012), and other coarse-resolution simulations using a similar variable GM scheme (Lovenduski et al., 2013). Spatially, the differing circulation response between the eddy parameterizations occurred principally in the Deacon cell between 40° and 60° S (Fig. 5c).

We note that the response of both the residual overturning and the surface CO_2 flux to wind changes was about 2.5 times smaller under the variable GM scheme than under the constant GM scheme over 1950 to 2010. The parameterization of mesoscale eddies is therefore a key determinant of the wind feedback on the ocean carbon sink. However the magnitude of the wind forcing itself is uncertain, to which we now turn.

4   The oceanic response to wind changes over 1980 to 2010 in six reanalyses

4.1   Comparison of reanalysis winds

To examine the uncertainty in the wind forcing of the ocean we compare six reanalyses over the period 1980 to 2010 (Table 1). The zonal mean wind speed climatologies show that the reanalyses differ significantly, particularly in the key region of the SH westerlies, which vary in strength by about 20 % amongst the products (Fig. 6a).

The reanalyses also differ significantly in their surface wind trends over 1980 to 2010 (Fig. 6b). The largest trends generally occur in the SH westerly jets. However, the reanalyses do not even agree on the sign of the trend. The NASA MERRA and NCEP

---

[1]With a typical isopycnal slope of 10^{-3} and the circumference of the Earth at Drake Passage latitudes of 25 × 10^6 m, a change of K_{GM} of 10^2 m^2 s^{-1} implies a change of eddy-induced overturning of 2.5 Sv, consistent with our model (Fig. 5b).

Full Screen / Esc

Printer-friendly Version

Interactive Discussion

CFSR westerly jets have negative trends, which is in disagreement with station based observations and may be due to changes in the type of data assimilated over time (Swart and Fyfe, 2012). Even amongst the remaining four reanalyses which exhibit a positive trend in the SH westerlies, the magnitude of the trends varies by more than three times. These uncertainties in the wind climatologies and trends leads to uncertainty in the ocean carbon response which we now consider.

4.2 The ocean carbon response to different reanalysis winds

We return to considering the net surface CO_2 fluxes, but this time over the period 1980 to 2010, and for six simulations each forced by monthly repeating 1980 winds from an individual reanalysis and all using the variable GM scheme (Fig. 7a). Each of these simulations produce a net atmosphere to ocean CO_2 flux within the observational uncertainty (Ciais et al., 2013).

Our primary interest lies in the influence of wind changes on the cumulative surface flux. The difference between simulations with evolving and fixed winds shows a large separation in time among reanalyses (Fig. 7b). The reanalyses with large positive trends in the SH westerly jet (20CR, R2) show a large reduction in the ocean carbon sink, reaching up to $0.11\,Pg\,yr^{-1}\,decade^{-1}$ over 1980 to 2010. In contrast, other reanalyses show significantly smaller trends in the surface flux (Table 2). In the case of the CFSR and MERRA winds, the trend is of the opposite sign indicating enhanced ocean carbon uptake due to historical wind changes, consistent with the large negative and possibly spurious trend in those products SH westerly jets. Even ignoring CFSR and MERRA, the remaining four reanalyses would indicate that there are significant uncertainties in the magnitude of the wind feedback on the ocean carbon sink over the historical period.

The CO_2 flux trends depend on the time-frame selected because of the large inter-annual variability present, but the general conclusion of a large uncertainty amongst products is robust regardless of the choice (Table 2). The flux trends due to surface wind forcing also depend quantitatively on the experimental design. For example, the

20CR wind-induced trends over 1980 to 2010 differ in the experiment using transient winds over 1871 to 2010 ($0.069\,\mathrm{Pg\,yr^{-1}\,decade^{-1}}$) compared to the experiment using transient winds over only 1980 to 2010 ($0.027\,\mathrm{Pg\,yr^{-1}\,decade^{-1}}$). Such a dependency on the onset date of transient winds makes the wind-product comparison experiments reported by Le Quéré et al. (2010) hard to interpret because each of their simulations was initialized at a different time. Our advance here was treating all simulations in a consistent manner over 1871 to 2010 which allows a direct comparison amongst the surface forcing products. The key result is that a large uncertainty exists in the trend of the historical surface CO_2 flux due to the choice of surface forcing.

5 Conclusions

Using the 20th Century Reanalysis to provide wind forcing we have produced an ocean biogeochemical model based estimate of ocean carbon uptake over 1871 to 2010. Our simulations show that wind changes have significantly reduced the ocean carbon sink since 1871. Particularly over 1950 to 2010 an intensification of the SH westerly wind jet increased the residual overturning circulation in the Southern Ocean, leading to an outgassing of natural CO_2 and a net reduction in the ocean carbon sink reaching about 8 to 9 Pg, or roughly 10 % of the total ocean uptake by 2010. Our simulations show that the response of the ocean circulation and the carbon cycle is sensitive to the parameterization of mesoscale eddies. With a variable eddy transfer coefficient the response to wind changes is about 2.5 times smaller than when using a fixed coefficient. We also showed that significant uncertainty exists in wind trends over the period 1980 to 2010 by comparing six reanalyses. Our simulations indicate that the influence of historical wind changes on ocean carbon uptake is highly uncertain and depends on the choice of surface wind forcing and eddy parameterization scheme.

Changes in the ocean carbon sink

N. C. Swart et al.

References

Böning, C., Dispert, A., Visbeck, M., Rintoul, S., and Schwarzkopf, F.: The response of the Antarctic Circumpolar Current to recent climate change, Nat. Geosci., 1, 864–869, doi:10.1038/ngeo362, 2008. 8025

5 Ciais, P., Sabine, C., Bala, G., Bopp., L., Brovkin, V., Canadell, J., Chhabra, A., DeFries, R., Galloway, J., Heimann, M., Jones, C., Le Quéré, C., Myneni, R., Piao, S., and Thornton, P.: Carbon and other biogeochemical cycles, in: Climate Change 2013: The Physical Science Basis. Contribution of Working Group I to the Fifth Assessment Report of the Intergovernmental Panel on Climate Change, edited by: Stocker, T., Qin, D., Plattner, G.-K., Tignor, M.,

10 Allen, S., Boschung, J., Nauels, A., Xia, Y., Bex, V., and Midgley, P., chap. 6, Cambridge University Press, Cambridge, UK, New York, USA, 2013. 8029, 8033, 8043

Compo, G. P., Whitaker, J. S., Sardeshmukh, P. D., Matsui, N., Allan, R. J., Yin, X., Gleason, B. E., Vose, R. S., Rutledge, G., Bessemoulin, P., Brönnimann, S., Brunet, M., Crouthamel, R. I., Grant, A. N., Groisman, P. Y., Jones, P. D., Kruk, M. C., Kruger, A. C.,

15 Marshall, G. J., Maugeri, M., Mok, H. Y., Nordli, Ø., Ross, T. F., Trigo, R. M., Wang, X. L., Woodruff, S. D., and Worley, S. J.: The TWentieth CEntury Reanalysis Project, Q. J. Roy. Meteor. Soc., 137, 1–28, doi:10.1002/qj.776, 2011. 8025, 8028, 8040

Dee, D. P., Uppala, S. M., Simmons, A. J., Berrisford, P., Poli, P., Kobayashi, S., Andrae, U., Balmaseda, M. A., Balsamo, G., Bauer, P., Bechtold, P., Beljaars, A. C. M., van de Berg, L.,

20 Bidlot, J., Bormann, N., Delsol, C., Dragani, R., Fuentes, M., Geer, A. J., Haimberger, L., Healy, S. B., Hersbach, H., Hólm, E. V., Isaksen, L., Kållberg, P., Köhler, M., Matricardi, M., McNally, A. P., Monge-Sanz, B. M., Morcrette, J.-J., Park, B.-K., Peubey, C., de Rosnay, P., Tavolato, C., Thépaut, J.-N., and Vitart, F.: The ERA-Interim reanalysis: configuration and performance of the data assimilation system, Q. J. Roy. Meteor. Soc., 137, 553–597,

25 doi:10.1002/qj.828, 2011. 8040

Eby, M., Zickfeld, K., Montenegro, A., Archer, D., Meissner, K. J., and Weaver, A. J.: Lifetime of anthropogenic climate change: millennial time scales of potential CO_2 and surface temperature perturbations, J. Climate, 22, 2501–2511, 2009. 8026

Eby, M., Weaver, A. J., Alexander, K., Zickfeld, K., Abe-Ouchi, A., Cimatoribus, A. A.,

30 Crespin, E., Drijfhout, S. S., Edwards, N. R., Eliseev, A. V., Feulner, G., Fichefet, T., Forest, C. E., Goosse, H., Holden, P. B., Joos, F., Kawamiya, M., Kicklighter, D., Kienert, H., Matsumoto, K., Mokhov, I. I., Monier, E., Olsen, S. M., Pedersen, J. O. P., Perrette, M., Philippon-

Changes in the ocean carbon sink

N. C. Swart et al.

Title Page

Abstract	Introduction
Conclusions	References
Tables	Figures

◀◀ ▶▶

◀ ▶

Back | Close

Full Screen / Esc

Printer-friendly Version

Interactive Discussion

Berthier, G., Ridgwell, A., Schlosser, A., Schneider von Deimling, T., Shaffer, G., Smith, R. S., Spahni, R., Sokolov, A. P., Steinacher, M., Tachiiri, K., Tokos, K., Yoshimori, M., Zeng, N., and Zhao, F.: Historical and idealized climate model experiments: an intercomparison of Earth system models of intermediate complexity, Clim. Past, 9, 1111–1140, doi:10.5194/cp-9-1111-2013, 2013. 8026

Farneti, R. and Gent, P. R.: The effects of the eddy-induced advection coefficient in a coarse-resolution coupled climate model, Ocean Model., 39, 135–145, doi:10.1016/j.ocemod.2011.02.005, 2011. 8026

Gent, P. and McWilliams, J.: Isopycnal mixing in ocean circulation models, J. Phys. Oceanogr., 20, 150–155, doi:10.1175/1520-0485(1990)020<0150:IMIOCM>2.0.CO;2, 1990. 8026

Gnanadesikan, A., Dixon, K. W., Griffies, S. M., Balaji, V., Barreiro, M., Beesley, J. A., Cooke, W. F., Delworth, T. L., Gerdes, R., Harrison, M. J., Held, I. M., Hurlin, W. J., Lee, H.-C., Liang, Z., Nong, G., Pacanowski, R. C., Rosati, A., Russell, J., Samuels, B. L., Song, Q., Spelman, M. J., Stouffer, R. J., Sweeney, C. O., Vecchi, G., Winton, M., Wittenberg, A. T., Zeng, F., Zhang, R., and Dunne, J. P.: GFDL's CM2 global coupled climate models. Part II: The baseline ocean simulation, J. Climate, 19, 675–697, doi:10.1175/JCLI3630.1, 2006. 8026

Gruber, N., Gloor, M., Mikaloff Fletcher, S., Doney, S., Dutkiewicz, S., Follows, M., Gerber, M., Jacobson, A., Joos, F., Lindsay, K., Menemenlis, D., Mouchet, A., Muller, S., Sarmiento, J., and Takahashi, T.: Oceanic sources, sinks, and transport of atmospheric CO_2, Global Biogeochem. Cy., 23, GB1005, doi:10.1029/2008GB003349, 2009. 8025

Kalnay, E., Kanamitsu, M., Kistler, R., Collins, W., Deaven, D., Gandin, L., Iredell, M., Saha, S., White, G., Woollen, J., Zhu, Y., Leetmaa, A., Reynolds, R., Chelliah, M., Ebisuzaki, W., Higgins, W., Janowiak, J., Mo, K. C., Ropelewski, C., Wang, J., Jenne, R., and Joseph, D.: The NCEP/NCAR 40-year reanalysis project, B. Am. Meteorol. Soc., 77, 437–471, doi:10.1175/1520-0477(1996)077<0437:TNYRP>2.0.CO;2, 1996. 8040

Kanamitsu, M., Ebisuzaki, W., Woollen, J., Yang, S.-K., Hnilo, J. J., Fiorino, M., and Potter, G. L.: NCEP–DOE AMIP-II reanalysis (R-2), B. Am. Meteorol. Soc., 83, 1631–1643, doi:10.1175/BAMS-83-11-1631, 2002. 8040

Le Quéré, C., Rödenbeck, C., Buitenhuis, E. T., Conway, T. J., Langenfelds, R., Gomez, A., Labuschagne, C., Ramonet, M., Nakazawa, T., Metzl, N., Gillett, N., and Heimann, M.: Saturation of the Southern Ocean CO_2 sink due to recent climate change, Science, 316, 1735–1738, doi:10.1126/science.1136188, 2007. 8024, 8025, 8029, 8030

Le Quéré, C., Takahashi, T., Buitenhuis, E. T., Rödenbeck, C., and Sutherland, S. C.: Impact of climate change and variability on the global oceanic sink of CO_2, Global Biogeochem. Cy., 24, GB4007, doi:10.1029/2009GB003599, 2010. 8025, 8029, 8030, 8034

Le Quéré, C., Andres, R. J., Boden, T., Conway, T., Houghton, R. A., House, J. I., Marland, G., Peters, G. P., van der Werf, G. R., Ahlström, A., Andrew, R. M., Bopp, L., Canadell, J. G., Ciais, P., Doney, S. C., Enright, C., Friedlingstein, P., Huntingford, C., Jain, A. K., Jourdain, C., Kato, E., Keeling, R. F., Klein Goldewijk, K., Levis, S., Levy, P., Lomas, M., Poulter, B., Raupach, M. R., Schwinger, J., Sitch, S., Stocker, B. D., Viovy, N., Zaehle, S., and Zeng, N.: The global carbon budget 1959–2011, Earth Syst. Sci. Data, 5, 165–185, doi:10.5194/essd-5-165-2013, 2013. 8024

Lenton, A., Tilbrook, B., Law, R. M., Bakker, D., Doney, S. C., Gruber, N., Ishii, M., Hoppema, M., Lovenduski, N. S., Matear, R. J., McNeil, B. I., Metzl, N., Mikaloff Fletcher, S. E., Monteiro, P. M. S., Rödenbeck, C., Sweeney, C., and Takahashi, T.: Sea–air CO_2 fluxes in the Southern Ocean for the period 1990–2009, Biogeosciences, 10, 4037–4054, doi:10.5194/bg-10-4037-2013, 2013. 8025, 8030

Lovenduski, N. S., Gruber, N., Doney, S. C., and Lima, I. D.: Enhanced CO_2 outgassing in the Southern Ocean from a positive phase of the Southern Annular Mode, Global Biogeochem. Cy., 21, GB2026, doi:10.1029/2006GB002900, 2007. 8024

Lovenduski, N. S., Gruber, N., and Doney, S. C.: Toward a mechanistic understanding of the decadal trends in the Southern Ocean carbon sink, Global Biogeochem. Cy., 22, GB3016, doi:10.1029/2007GB003139, 2008. 8025, 8029, 8030

Lovenduski, N. S., Long, M. C., Gent, P. R., and Lindsay, K.: Multi-decadal trends in the advection and mixing of natural carbon in the Southern Ocean, Geophys. Res. Lett., 40, 139–142, 2013. 8025, 8032

Marshall, J. and Radko, T.: Residual-mean solutions for the Antarctic Circumpolar Current and its associated overturning circulation, J. Phys. Oceanogr., 33, 2341–2354, doi:10.1175/1520-0485(2003)033<2341:RSFTAC>2.0.CO;2, 2003. 8031

Meredith, M. P., Naveira Garabato, A. C., Hogg, A. M., and Farneti, R.: Sensitivity of the overturning circulation in the Southern Ocean to decadal changes in wind forcing, J. Climate, 25, 99–110, doi:10.1175/2011JCLI4204.1, 2011. 8032

Morrison, A. K. and Hogg, A. M.: On the relationship between Southern Ocean overturning and ACC transport, J. Phys. Oceanogr., 43, 140–148, doi:10.1175/JPO-D-12-057.1, 2012. 8032

Full Screen / Esc

Printer-friendly Version

Interactive Discussion

Rienecker, M. M., Suarez, M. J., Gelaro, R., Todling, R., Bacmeister, J., Liu, E., Bosilovich, M. G., Schubert, S. D., Takacs, L., Kim, G.-K., Bloom, S., Chen, J., Collins, D., Conaty, A., da Silva, A., Gu, W., Joiner, J., Koster, R. D., Lucchesi, R., Molod, A., Owens, T., Pawson, S., Pegion, P., Redder, C. R., Reichle, R., Robertson, F. R., Ruddick, A. G., Sienkiewicz, M., and Woollen, J.: MERRA: NASA's Modern-Era Retrospective Analysis for Research and Applications, J. Climate, 24, 3624–3648, doi:10.1175/JCLI-D-11-00015.1, 2011. 8040

Saha, S., Moorthi, S., Pan, H.-L., Wu, X., Wang, J., Nadiga, S., Tripp, P., Kistler, R., Woollen, J., Behringer, D., Liu, H., Stokes, D., Grumbine, R., Gayno, G., Wang, J., Hou, Y.-T., Chuang, H.-Y., Juang, H.-M. H., Sela, J., Iredell, M., Treadon, R., Kleist, D., Van Delst, P., Keyser, D., Derber, J., Ek, M., Meng, J., Wei, H., Yang, R., Lord, S., Van Den Dool, H., Kumar, A., Wang, W., Long, C., Chelliah, M., Xue, Y., Huang, B., Schemm, J.-K., Ebisuzaki, W., Lin, R., Xie, P., Chen, M., Zhou, S., Higgins, W., Zou, C.-Z., Liu, Q., Chen, Y., Han, Y., Cucurull, L., Reynolds, R. W., Rutledge, G., and Goldberg, M.: The NCEP climate forecast system reanalysis, B. Am. Meteorol. Soc., 91, 1015–1057, doi:10.1175/2010BAMS3001.1, 2010. 8040

Sarmiento, J. L., Gloor, M., Gruber, N., Beaulieu, C., Jacobson, A. R., Mikaloff Fletcher, S. E., Pacala, S., and Rodgers, K.: Trends and regional distributions of land and ocean carbon sinks, Biogeosciences, 7, 2351–2367, doi:10.5194/bg-7-2351-2010, 2010. 8024

Schmittner, A., Oschlies, A., Matthews, H. D., and Galbraith, E. D.: Future changes in climate, ocean circulation, ecosystems, and biogeochemical cycling simulated for a business-as-usual CO_2 emission scenario until year 4000 AD, Global Biogeochem. Cy., 22, GB1013, doi:10.1029/2007GB002953, 2008. 8026

Son, S.-W., Gerber, E. P., Perlwitz, J., Polvani, L. M., Gillett, N. P., Seo, K.-H., Eyring, V., Shepherd, T. G., Waugh, D., Akiyoshi, H., Austin, J., Baumgaertner, A., Bekki, S., Braesicke, P., Brühl, C., Butchart, N., Chipperfield, M. P., Cugnet, D., Dameris, M., Dhomse, S., Frith, S., Garny, H., Garcia, R., Hardiman, S. C., Jöckel, P., Lamarque, J. F., Mancini, E., Marchand, M., Michou, M., Nakamura, T., Morgenstern, O., Pitari, G., Plummer, D. A., Pyle, J., Rozanov, E., Scinocca, J. F., Shibata, K., Smale, D., Teyssèdre, H., Tian, W., and Yamashita, Y.: Impact of stratospheric ozone on Southern Hemisphere circulation change: a multimodel assessment, J. Geophys. Res.-Atmos., 115, D00M07, doi:10.1029/2010JD014271, 2010. 8028

Swart, N. C. and Fyfe, J. C.: Observed and simulated changes in the Southern Hemisphere surface westerly wind-stress, Geophys. Res. Lett., 39, L16711, doi:10.1029/2012GL052810, 2012. 8025, 8028, 8033

Printer-friendly Version

Interactive Discussion

Thompson, D. W. J. and Solomon, S.: Interpretation of recent Southern Hemisphere climate change, Science, 296, 895–899, doi:10.1126/science.1069270, 2002. 8028

Wanninkhof, R., Park, G. -H., Takahashi, T., Sweeney, C., Feely, R., Nojiri, Y., Gruber, N., Doney, S. C., McKinley, G. A., Lenton, A., Le Quéré, C., Heinze, C., Schwinger, J., Graven, H., and Khatiwala, S.: Global ocean carbon uptake: magnitude, variability and trends, Biogeosciences, 10, 1983–2000, doi:10.5194/bg-10-1983-2013, 2013. 8024, 8025, 8030

Weaver, A., Eby, M., Wiebe, C., Bitz, M., Duffy, C., Ewen, T.L., Fanning, A., Holland, M., MacFadyen, A., Matthews, H., Meissner, K., Saenko, O., Schmittner, A., Wang, H., and Yoshimori, M.: The UVic Earth System Climate Model: model description, climatology, and applications to past, present and future climates, Atmos. Ocean, 39, 1–68, doi:10.1080/07055900.2001.9649686, 2001. 8026

Zickfeld, K., Fyfe, J., Eby, M., and Weaver, A.: Comment on "Saturation of the Southern Ocean CO$_2$ sink due to recent climate change", Science, 319, 5863, doi:10.1126/science.1146886, 2008. 8025

Changes in the ocean carbon sink

N. C. Swart et al.

Table 1. List of reanalysis surface winds (speed and stress fields) used in this study. 20CR is an ensemble reanalysis, and here we have used the ensemble mean. It should be noted that the publicly available 20CR ensemble-mean wind-speeds were incorrectly calculated. For application here we have recomputed the ensemble mean speed.

Name	Abbreviation	Reference
NCEP/NCAR Reanalysis 1	R1	Kalnay et al. (1996)
NCEP/DOE Reanalysis 2	R2	Kanamitsu et al. (2002)
Twentieth Century Reanalysis v2	20CR	Compo et al. (2011)
ERA-Interim Reanalysis	ERA-Int	Dee et al. (2011)
NCEP CFSR	CFSR	Saha et al. (2010)
NASA MERRA	MERRA	Rienecker et al. (2011)

Table 2. Trends in net surface CO_2 fluxes ($Pg\,yr^{-1}\,dec.^{-1}$). Trends that are statistically significant at the 5 % level are shown in bold. A negative trend indicates an enhanced ocean carbon sink. Total refers to the net global surface CO_2 flux trend in the simulation. Wind refers to the surface CO_2 flux trend due to wind forcing, calculated as the trend in the TRANSIENT minus FIXED simulation. The 1980–2010 simulations were each done with the variable GM coefficient.

Forcing	1871–2010 Total	1871–2010 Wind	1950–2010 Total	1950–2010 Wind	1980–2010 Total	1980–2010 Wind	1990–2010 Total	1990–2010 Wind
1871–2010 simulations								
20CR constant GM	**−0.117**	**0.028**	**−0.303**	**0.023**	**−0.147**	0.075	−0.137	0.086
20CR variable GM	**−0.111**	**0.016**	**−0.279**	0.009	**−0.135**	0.069	−0.142	0.065
1980–2010 simulations								
R1					**−0.153**	**0.102**	**−0.185**	**0.123**
R2					**−0.177**	**0.112**	**−0.286**	0.064
20CR					**−0.237**	0.027	**−0.304**	0.020
ERA-Int					**−0.206**	0.060	**−0.218**	0.096
CFSR					**−0.318**	−0.041	**−0.238**	0.101
MERRA					**−0.319**	−0.069	**−0.309**	−0.010
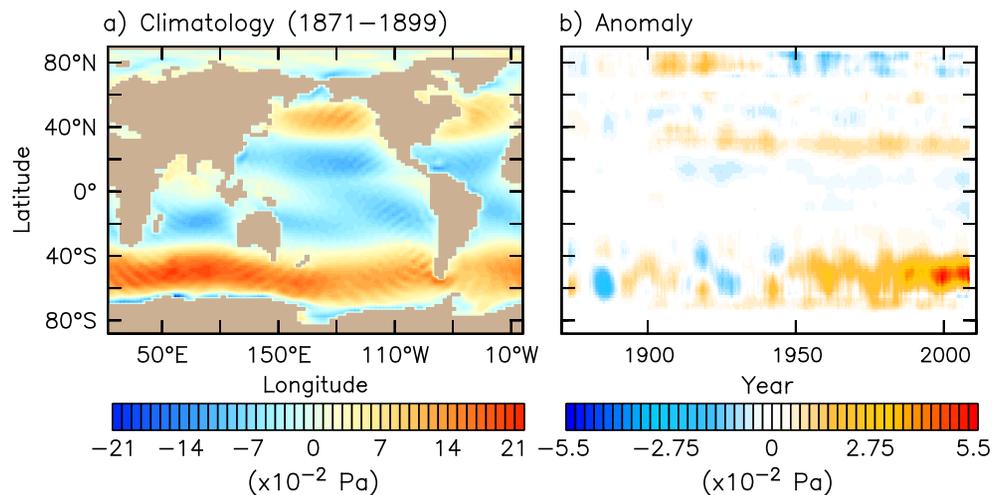
Figure 1. (a) The surface zonal wind-stress climatology of 20CR over 1871 to 1899 and **(b)** temporal changes in zonal-mean stress relative to the climatology.
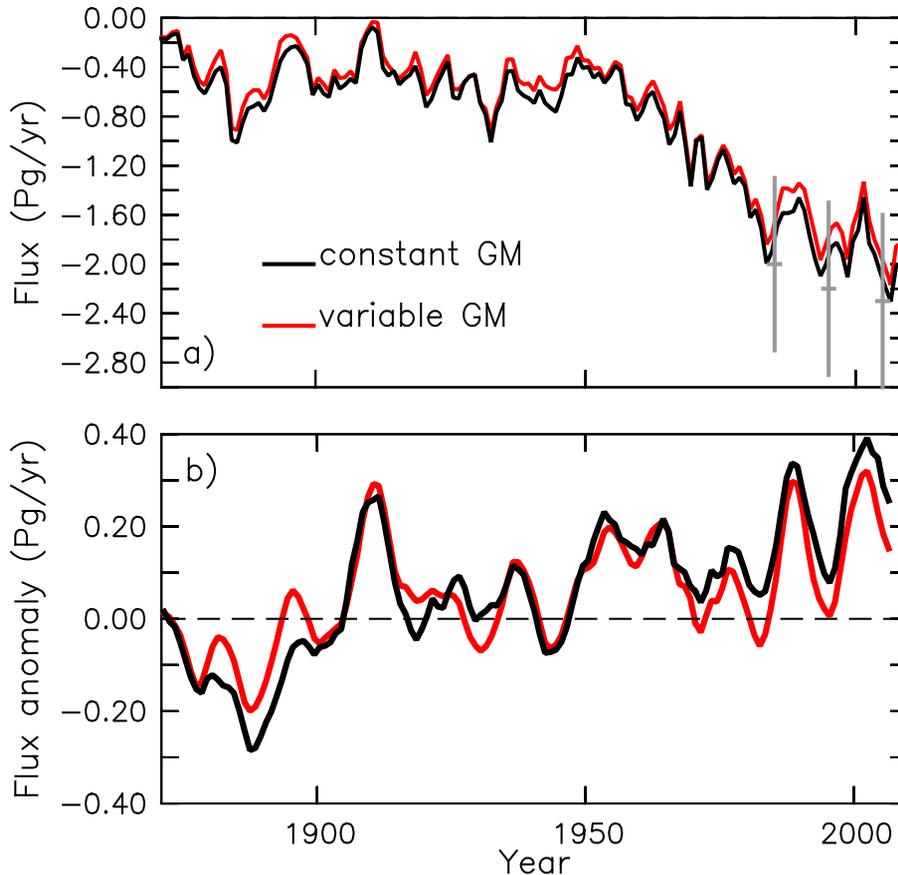
Figure 2. (a) Global net sea to air flux of CO_2 with time-evolving 20CR winds and **(b)** the surface flux anomaly due to the effect of time-evolving winds, computed as the difference between runs with time evolving and fixed winds. Fluxes are positive out of the ocean. The grey bars in **(a)** are observational estimates of the net flux (Ciais et al., 2013).

Full Screen / Esc

Printer-friendly Version

Interactive Discussion
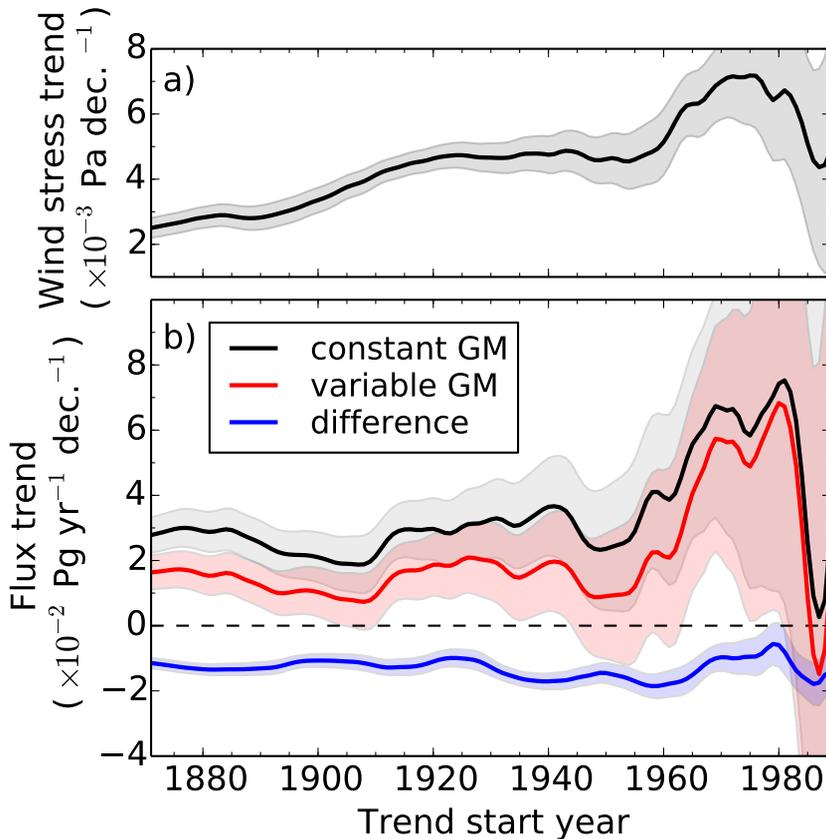
Figure 3. (a) The rolling linear trend in the surface wind-stress averaged zonally and over 40–60° S. **(b)** The rolling trend in the sea air CO_2 flux anomaly due to wind changes for the constant and variable GM simulations, as well as the difference trend between the two. The trends are calculated over the period with a start-year which rolls forward from 1871 to 1990 and an end year of 2010. The solid lines show the trend and the shaded envelopes are the 5 to 95 % confidence interval.
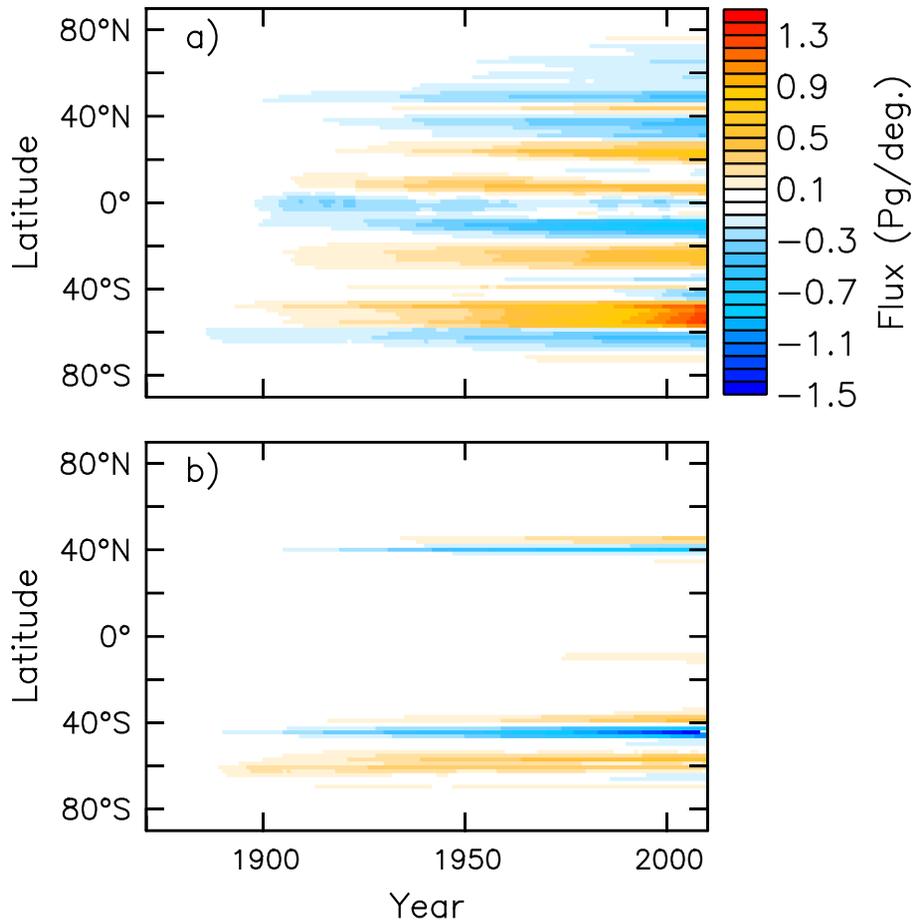
Figure 4. (a) The cumulative zonal-mean surface CO_2 flux anomaly over 1871 to 2010 due to the effect of time-evolving winds for the constant GM experiment (TRANSIENT minus FIXED) and **(b)** difference in the flux anomaly between the variable and constant GM experiments.
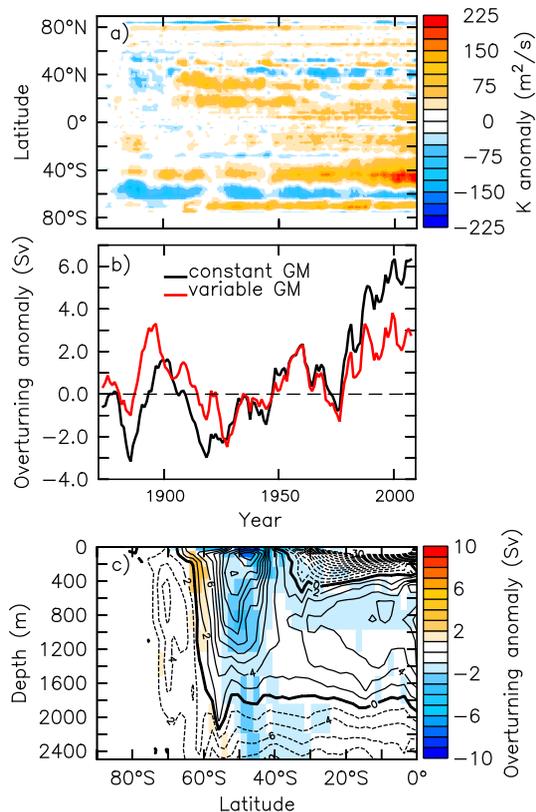
Figure 5. (a) The zonal-mean anomaly of eddy diffusivity due to the effect of time-evolving winds in the variable GM experiment (TRANSIENT minus FIXED); **(b)** wind-induced changes in the Southern Ocean residual overturning circulation and **(c)** in shading the difference in the residual overturning streamfunction between the variable and constant GM experiments with transient winds, averaged over 2000 to 2010, with contours giving the overturning streamfunction in the constant GM experiment over the same period.

Full Screen / Esc

Printer-friendly Version

Interactive Discussion
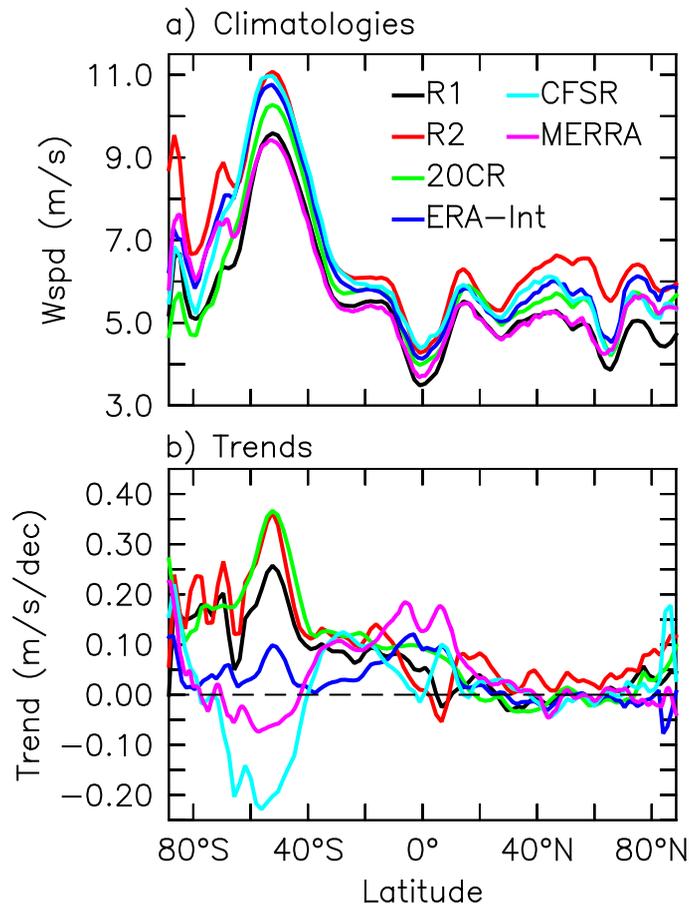
Figure 6. (a) Zonal-mean 10 m wind-speed climatologies over 1980 to 2010 in six reanalyses and **(b)** zonal-mean wind-speed trends over the same period. Wind-speeds are compared rather than surface stress fields, because the later are sensitive to the choice of drag coefficient.

Full Screen / Esc

Printer-friendly Version

Interactive Discussion
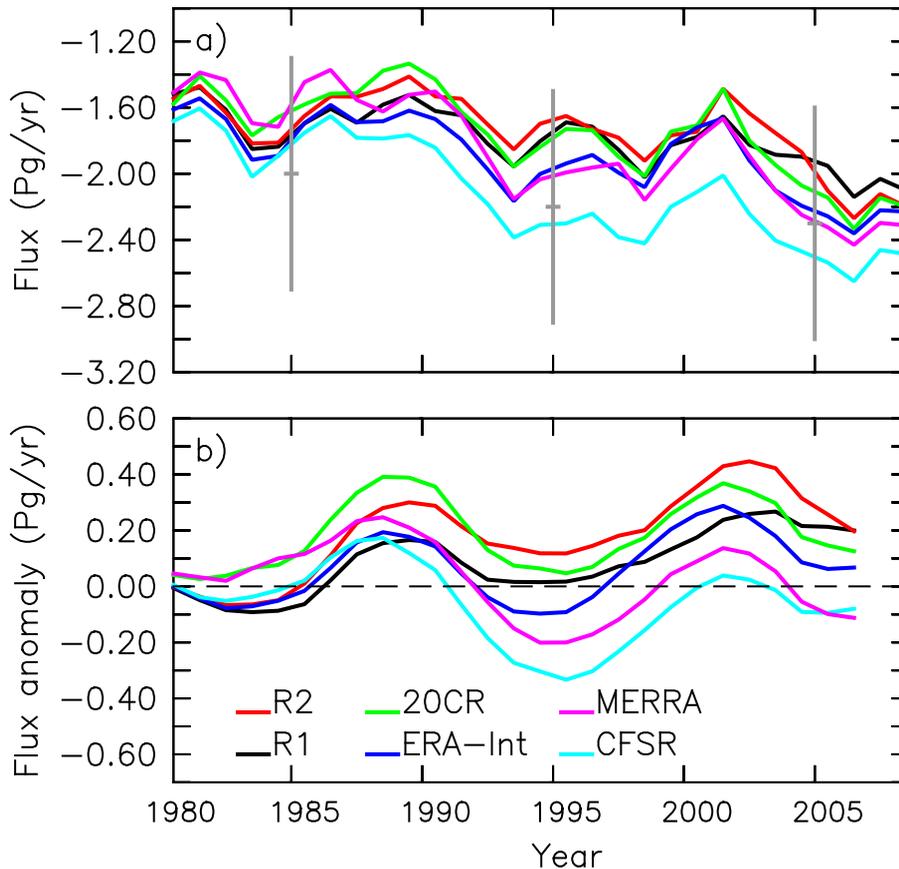
Figure 7. (a) Global net sea to air flux of CO_2 since 1980 for six runs with different reanalysis winds and **(b)** the surface flux anomaly due to the effect of time-evolving winds, computed as the difference between runs with time-evolving and fixed winds. Fluxes are positive out of the ocean.

Title Page

Abstract | Introduction

Conclusions | References

Tables | Figures

Back | Close

Full Screen / Esc

Printer-friendly Version

Interactive Discussion